RECONSTRUCTION ALGORITHM FOR PHOTOACOUSTIC TOMOGRAPHY (PAT) IMAGING SYSTEM OF SPHERICAL TRANSDUCER ARRAY.

A Project Report Submitted

in Partial Fulfilment of the Requirements

for the Degree of

MASTER OF SCIENCE

in

Physics

by

ALFAZAL M

Roll No. IMS12011

to

SCHOOL OF PHYSICS

INDIAN INSTITUTE OF SCIENCE EDUCATION AND RESEARCH THIRUVANANTHAPURAM – 695016, INDIA

April 2017

CERTIFICATE

This is to verify that the work contained in this project report entitled "**Reconstruction algorithm for photoacoustic tomography (PAT) imaging system of spherical transducer array**" submitted by **Alfazal M (Roll No. IMS12011)** to Indian Institute of Science Education and Research Thiruvananthapuram (IISER – TVM) towards the partial requirement of **Master of Science(MS)** in **Physics** has been carried out by him under my supervision and that it has not been submitted elsewhere for the award of any degree.

Place : Thiruvananthapuram – 695 016
Date: April 2017

Dr. Mayanglambam Suheshkumar Singh
Project Supervisor
School of Physics(SoP),IISER-TVM
Thiruvananthapuram,Kerala

ACKNOWLEDGEMENT

I would like to express my special thanks of gratitude to my project supervisor Dr. M. Suheshkumar Singh, Assistant Professor, School of Physics, IISER TVM, for giving me an opportunity to work with him. I would like to thank all my lab mates, Miss Anjali Thomas, Mr. Balvinder Pal Singh Bindra and Miss Rinsa S.R., for their kind support and help.

I'm thankful to my family members and friends who helped me to be stay motivated and completing this work.

ABSTRACT

There is a limited understanding of metabolism, spatiotemporal dynamics, and physiological changes – of neurons deep inside the brain in intact cells. This lack of knowledge is due to the challenges that remain in development of imaging technologies with achievable spatial resolution ($\sim\mu m$) at depth ($\sim cms$) for neuro-imaging beyond cerebral cortex. This research project aims to: (1) develop reconstruction algorithm of a imaging system for a 4D microscopic-resolution Photoacoustic tomography (4D μ-PAT) with resolution($\sim 200\mu m$) at depth ($\sim cm$) – that has been being undertaken for development by our research group and (2) evaluate the performance of a specially designed ultrasound detection unit – in which an array of ultrasound transducer (512) elements are uniformly and densely distributed over a section of spherical surface – that is employed in the imaging system. The reconstruction algorithm targets to achieve spatial resolution ($\sim 200\mu m$) with imaging depth ($\sim cms$). Numerical simulation studies are carried out – both in numerical phantoms and raw data obtained (for human hair sample) using photoacoustic microscopy – to evaluate the performance of the algorithm. The study shows that the algorithm achieves spatial resolution $\sim 200\mu m$. various image filtering techniques – such as thresholding and born ratio technique – are studied for improving the quality of the reconstructed images. The results demonstrate that the above mentioned techniques successfully remove the noise from the background and subsequently, improve the contrast of the reconstructed image. This study not only opens a unique avenue for mapping and hence, understanding the neurophysiology deep inside the brain. This will also be of great impact on drug design and development for treatment of neurological disorders.

CONTENTS

LIST OF FIGURES

1. INTRODUCTION

For diagnosis and therapeutic treatment of neuronal disorders – other than understanding of metabolism, spatiotemporal dynamics and physiological activities – non-invasive and non-destructive scanning device with spatial resolution (~μm) and imaging depth (~cm) are demanded. The conventional super resolution imaging such as electron and atomic microscopy that achieve spatial resolution (~nm - A^{o}) beyond the optical diffraction limit. They are not suitable for biomedical applications because of the limited imaging depth (~nm suitable only for surface or ultra-thin film imaging). For overcoming the restriction of imaging depth, optics based microscopy techniques – confocal and fluorescence-based two-photon microscopies – are conventionally utilized even though having limited optical imaging depth (~0.5-1.0mm) and resolution (~nm). However, these technologies demand a thin slice of the sample being introduced in the sample holder and consequently, these technologies do not permit to study the dynamics and characterization of tissues deep inside the body. Due to this limitation, it has been an area of active research to develop non-invasively and non-destructive imaging techniques that provide high imaging depth with high spatial resolution. One of the promising technique for studying in depth tissues in microscopic resolution is the photoacoustic modality [1-4, 5] – which is emerging and rapidly growing – that combines the advantageous features of both microscopy (with resolution ~μm and depth ~mm) and tomography (with resolution ~500μm and depth ~cms).

Photoacoustic microscopy gives higher spatial resolution (but low penetration depth and low temporal resolution) while PAT gives higher temporal resolution (but low spatial resolution). For achieving real time imaging at microscopic resolution, we need imaging to be performed at the same time with high spatial and temporal resolution. Our research group aim at design and development of 4D μ-PAT that facilitates the following unique features: (1) improving temporal resolution (>10$msec$) using higher pulse repetition frequency (PRF~100Hz), (2) image contrast employing Born-ratio technique[6], and (3) improving spatial resolution by increasing the number density and the operating frequency of the (ultrasound) detectors. This imaging technique – that not only combines the advantageous features of the high resolution of ultrasound imaging and the high contrast of optical imaging but also the high resolution of PAM and the high penetration depth of PAT. The objective of this project is, mainly, for development of a reconstruction algorithm that is to be adapted to this imaging technology through. Studies are carried both in numerical phantom as well as in raw data obtained from photo acoustic microscopy (PAM). Also several imaging techniques – thresholding, and Born-Ratio techniques were studied in order to improve the performance of

the reconstruction algorithm, i.e. to increase the contrast of the image and remove the background noise. The results show that these imaging techniques successfully remove the background noise and improve the contrast of the reconstructed image.

From technological aspects, in PAT a tissue sample is illuminated by a narrow pulse (pulse width ~5-10nsec) of electromagnetic radiation in the visible or near infrared region (NIR) range. This illuminated tissue sample absorbs the light energy and some part of the energy is converted into heat that causes the thermo-elastic expansion of the tissue. Subsequently, it produces a broadband ultrasonic waves. The ultrasound waves on exiting the tissue surface is detected using an array of ultrasound transducer detectors being kept on the tissue boundary. From this array of detected ultrasonic waves, a reconstruction technique is employed to recover images (2D or 3D) of the tissue. In our experimental system (as shown in figure 1) – that is under construction –, we are employing OPO pulse laser (pulse width ~5*nsec*, pulse energy ~25*mJ*, optical wavelength ~700-1000*nm*, and pulse repetition frequency (PRF~100-200*Hz*)) for generating the high-intensity laser beam that is coupled with a multimode optical fibre to illuminate the tissue sample of interest. A specially designed transducer unit – in which an array of transducer elements (512 elements instead of 256 as done by Razansky *et.al.*[1]) is densely distributed over a (concave) hemispherical surface – will be employed. The US-signals from the individual US-elements will be acquired in parallel using a DAQ-system having 512 channels and transferred to a high performance computer system – for post processing and reconstruction – that is controlled by the triggering output of the OPO-laser source enabling to acquire one image-frame in each laser-pulse excitation, i.e., the achievable frame rate of the system is given by the PRF (~100-200Hz) of the laser source. For our simulation study being carried out in this project, k-wave Toolbox [7] (an open source acoustic toolbox in MATLAB) developed by Bradley Treeby *et. al.* is used. Studies are carried out both in numerical phantom as well as data obtained from photoacoustic microscopy for human hair sample. We employ MATLAB software for our study. Section 3 gives the detail of the numerical simulation studies while Section 4 presents the results of our studies with conclusion in Section 5.

2. THEORY

Fundamentally, photoacoustic imaging is based on photoacoustic effect [8] – propounded by Alexander Graham Bell in 1880 – that is the generation of sound waves due to absorption of light, at short duration, in a sample material. When a short pulse of light is irradiating a sample material, due to absorption of light and subsequent rapid heating of irradiated sample material, it induces thermo-elastic expansion. Consequently, generation of mechanical wave (known as photoacoustic) is resulted. Photoacoustic amplitude is proportional to optical absorption. Non-absorbing components present no background due to this PAT provides back ground free detection. The fractional volume expansion $\Delta V / V$ is given by [9]:

$$\frac{\Delta V}{V} = -k\Delta p + \beta\Delta T \ , \tag{1}$$

where k is the isothermal compressibility β is the thermal coefficient of volume expansion, and p and T denote pressure (measured in Pascal) and temperature (in Kelvin), respectively.

When the fractional change in volume is negligible under rapid heating, the pressure rise immediately after the illumination can be derived from Equation 2 [9] as:

$$p_o = \frac{\beta\Delta T}{K} = \frac{\beta}{k\rho C_v} A_e, \tag{2}$$

where ρ denotes mass density C_v denotes specific heat capacity at constant volume, A_e is the optical absorption.

Approximately, a temperature rise of $1mk$ results in a pressure rise of $800Pa$ [5] , which is above the (typical) noise level from background. For propagation of acoustic waves in a homogenous and non-absorbing medium, distribution of acoustic properties can be written – in terms of equation of motion (Equation 3), equation of continuity (Equation 4) and equation of state (Equation 5) – as [7]:

$$\frac{\partial}{\partial t} u(\vec{r}, t) = -\frac{1}{\rho_0(x)} \nabla p(\vec{r}, t), \tag{3}$$

$$\frac{\partial}{\partial t} \rho(\vec{r}, t) = -\rho_0(\vec{r}) \nabla p(r, t), \tag{4}$$

$$p(\vec{r}, t) = c_0(\vec{r})^2 \rho(\vec{r}, t), \tag{5}$$

where $u(\vec{r},t)$ represents acoustic particle velocity at position vector ($\vec{r}$) inside the imaging region at the instant (t), $\rho(x)$ and $\rho_0(x)$ represents the acoustic and ambient densities, $P(\vec{r},t)$ is the acoustic pressure and c_0 is the sound speed. The equation governing the propagation of acoustic waves with the associated initial conditions are given by [10,11] Equation 6.

$$\left(\frac{d^2}{dt^2} - c(\vec{r})^2\rho(\vec{r})\nabla.\left(\frac{1}{\rho(\vec{r})}\nabla\right)\right)p(\vec{r},t) = 0, \quad (6)$$

Initial conditions are given by Equation 7 & 8 .

$$p(\vec{r},t)\,|_{t=0} = p_o\,(\vec{r})\,, \quad (7)$$

$$u(\vec{r},t)|_{t=0} = 0\,. \quad (8)$$

The forward propagation of the acoustic waves is simulated based on these equation. Acoustic signals are detected at multiple positions around the object using a ultrasound transducer array. Our aim is to get the initial pressure distribution $P_0(\vec{r})$ inside the domain of interest, say tissue sample for which time a reversal method is implemented. In time reversal imaging, the pressure values over the detection surface for series of time steps $t = 0$ to $t = T$ is used. In this case, the initial pressure is set to zero [12] (Equation 9).

$$p(r,t)|_{t=0} = 0, \quad (9)$$

The pressure value at a point $(\vec{r})$ over the detection surface for time steps from $t=T$ to $t=0$ is given by Equation 10.

$$p(\vec{r}_s,t) = p_m(\vec{r}_s, T-t) \quad (10)$$

where p_m is the recorded acoustic measurement in the forward problem. Reconstruction is performed using the recorded pressure data in time reversed order enforced as a Dirichlet boundary condition [13, 14] .

3. SIMULATION OF PHOTOACOUSTIC TOMOGRAPHY

For simulating PAT in MATLAB an open source toolbox K-Wave in MATLAB software is used. Initial pressure distribution, characteristics of medium the position and structure of detecting system are described as 3D matrices for the simulation of acoustic wave detection in the US transducer employed in our experimental system (Figure 1). The detection surface is described as a binary matrix. Time evolution of the wave field propagating in to the imaging region is treated as a forward problem with zero initial condition, .i.e. in this forward problem zero pressure will be given to all voxels. In the propagation of acoustic pressure to imaging domain this data will be treated as a time varying Dirichlet boundary condition [3, 4]. Reconstruction is performed and pressure distribution in the imaging region at time t=T will be obtained which is the initial pressure distribution in the first forward problem.

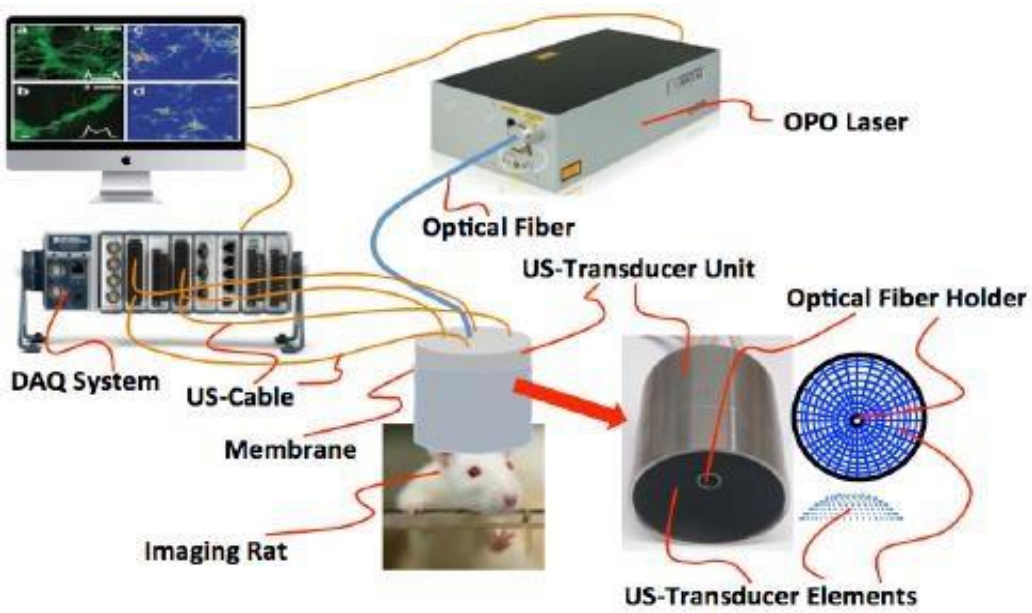

Figure 1: Design of experimental setup. DAQ system having 512 channels acquires data from the individual 512 transducer elements and data is transferred to a high performance computer system. Computer system is controlled by the OPO laser unit in order to acquire one image-frame in each laser pulse excitation.

3.1 MODELLING OF GENERATION OF THE PHOTOACOUSTIC WAVES IN 3D

The initial laser induced pressure distribution is created by a 3D images in k-wave toolbox. In the numerical simulation, this 3D image is treated as distribution of the strength of the initial photo acoustic waves as the source points. Series of time steps from $t=0$ to $t=T$ (T is the time taken by the acoustic waves from the source point to exiting the imaging region) are specified before doing the numerical simulation. The corresponding time array is 1617 steps and the step size is set to 50*ns*). Acoustic values are noted in the detection system, for this time steps only. Temporal resolution of the simulation is mainly determined by difference between these (consecutive) time steps. Simulation of PAT is employed for two types of initial acoustic sources. Two spherical structure as initial acoustic source and 3D image of hair sample as initial acoustic source (3D image created from acoustic data obtained for the hair sample using PAM).

3.2 MODELLING OF DETECTION OF THE PHOTOACOUSTIC SIGNAL WITH SPHERICAL 512 ELEMENT TRANSDUCER ARRAY AS AN US SENSOR UNIT

In K-wave toolbox, the sensor mask is described as a binary input matrices. For simulation in 3D, the input matrix for sensor mask is Nx*Ny*Nz in size, where Nx, Ny and Nz are the number of pixels in x-, y- and z-axes respectively. To model the transducer structure, an array of 512 identical detectors is evenly distributed along a spherical cap (diameter, 72*mm*)

with covering angle 140° (as shown in Figure 2(a)). This transducer structure of 512 elements is used to collect the data for acoustic waves originated from the source in the simulation. After reconstruction is performed, the acoustic pressure at each voxels in this detection surface for time steps *t=0* to *t=T* is obtained as a matrix. The transducer – that is going to be employed in our experimental system – has only 512 sensor elements. In our simulation study, acoustic pressure values – at all the voxels that lie in the region of each sensor element – are averaged. And this each averaged value is treated as a single acoustic measurement recorded by a sensor element in the transducer array. Sensor array gives 512 voxels corresponding to each sensor element and the reconstruction is performed using this averaged sensor data.

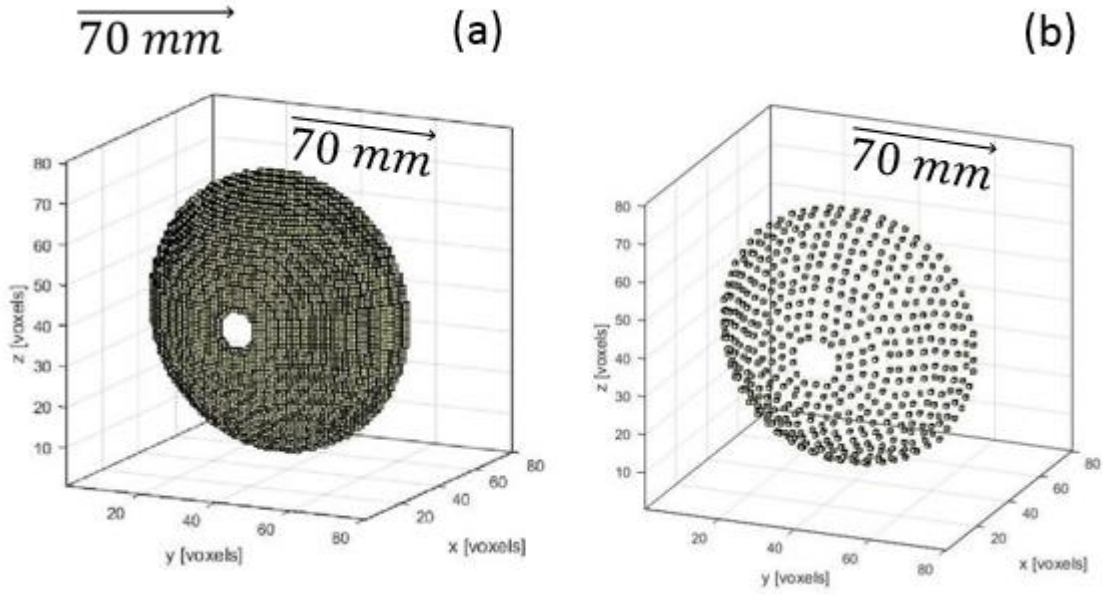

Figure 2: (a) Detecting system modelled – obtained with discretisation for numerical simulation with Nx =140, Ny =140 , and Nz =140 – in k-wave to detect acoustic signals from the acoustic source. (b) Sensor arrays of US transducer unit with 512 elements (for reconstruction) – similar to that employing in the experimental system – is modelled in k-wave.

3.3 SIMULATION OF ACOUSTIC WAVES FROM HAIR SAMPLE & RECONSTRUCTION OF HAIR SAMPLE

Numerical simulation study of a sample (numerical) of two spherical (acoustic) sources – separated by 500*um* – is carried out and the image of the spherical structures is reconstructed successfully with reconstruction technique mentioned above. Our experiment aims to develop 4D microscopic-resolution photoacoustic tomography (4D μ-PAT) imaging system that will enable to study the spatiotemporal dynamics of neurons in real time. The simulation study for the two spherical acoustic sources is performed without any noises and the source structures were trivial. As a step towards the simulation of Photoacoustic tomography of neurons, simulation of Photoacoustic tomography (PAT) with human hair sample as a source of acoustic

waves is carried out. Data obtained for human hair sample using photoacoustic microscopy (PAM) is rearranged and recreated as a matrix in MATLAB. And this matrix is used as source of acoustic waves in k-wave simulation toolbox.

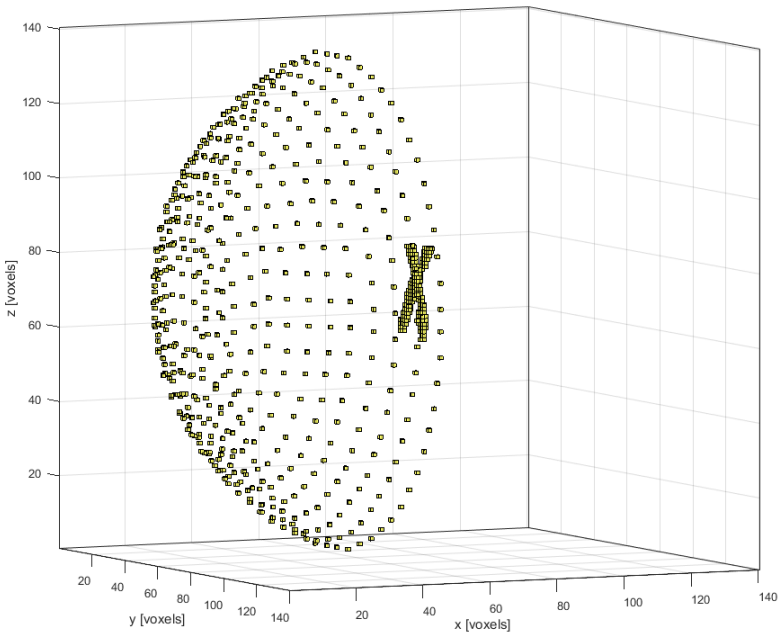

Figure 3: Hair sample as a source of acoustic waves (transducer array with 512 sensor elements is also shown). 3D hair sample image is placed near to the centre of spherical transducer structure.

4. RESULTS AND DISCUSSION

The results obtained for the reconstruction of a two spherical acoustic sources of radius $250\mu m$ with a separation of $500\mu m$ (and discretizing the imaging region with voxels of size 250 μm) along the axis of spherical cap is shown in Figure 4(a)&(c). 3D images are generated for both initial source and pressure distribution by employing AMIRA- software where a sequence of 2D images corresponding to each plane fixing along z-axis is used. The line plot of acoustic measurement on a plane passing through the source and parallel to xy-plane is given in Figure 4 (b) And (d) for both initial source and reconstructed initial pressure distribution respectively. Simulation for the reconstruction of a two spherical acoustic sources of radius 500 *um* with a separation of 500 *um* (and discretizing the imaging region with voxels of size 500 *um*) perpendicular to the axis of spherical cap (transducer array) is performed. As the result shows

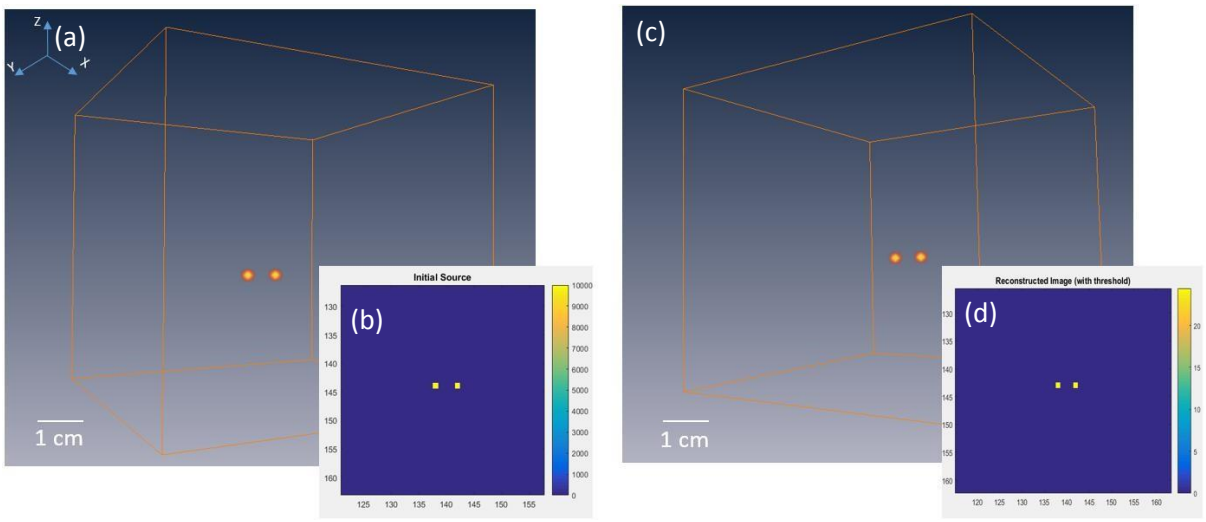

Figure 4 :(a) 3D image of initial acoustic source using AMIRA-software. (b) Cross section passing through initial source is plotted. (c) 3D image of reconstructed initial pressure distribution using AMIRA-software. (d) Plane passing through source is plotted for reconstructed pressure distribution. For acoustic sources 250 um in size and separated by 500*um*.

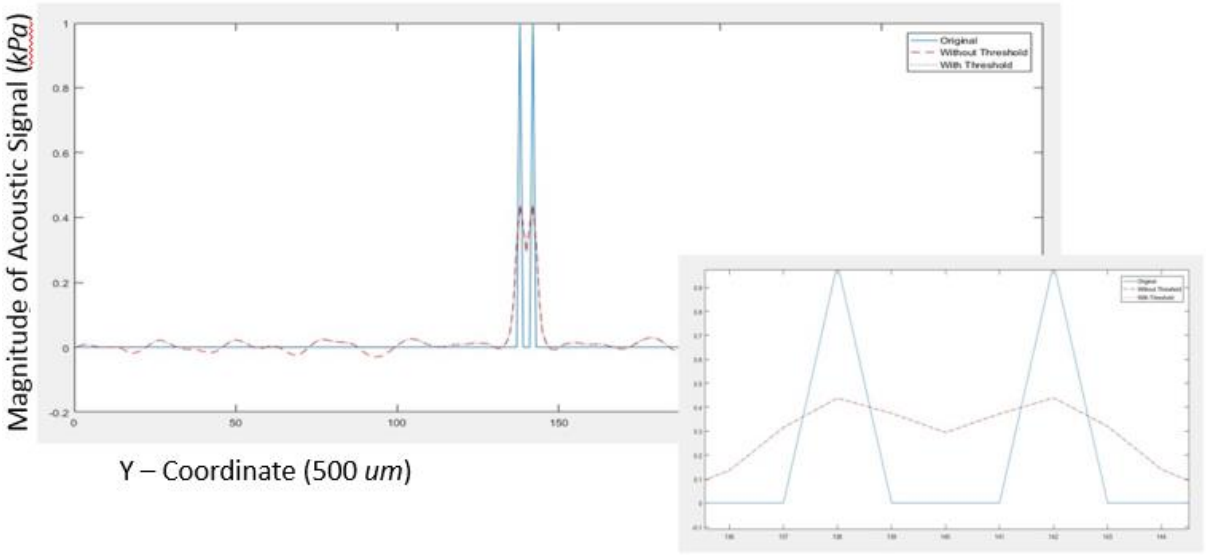

Figure 5: Line plot of measurement in the reconstructed acoustic distribution. Acoustic sources are separated by 500*μm* along the direction perpendicular to the transducer. The axes of acoustic magnitude and Y-coordinates are labelled.

acoustics sources are not resolved when they are placed with a separation 500 *um* along the axis of transducer array. The acoustic source that is far from transducer array and obscured by the other acoustic source is not reconstructed well. This is because of overshadowing of the PA-signal arising from the source – situated at the back side – by the signal from the object in front. This is a common challenge faced with photoacoustic tomography as well as in ultrasound imaging technology.

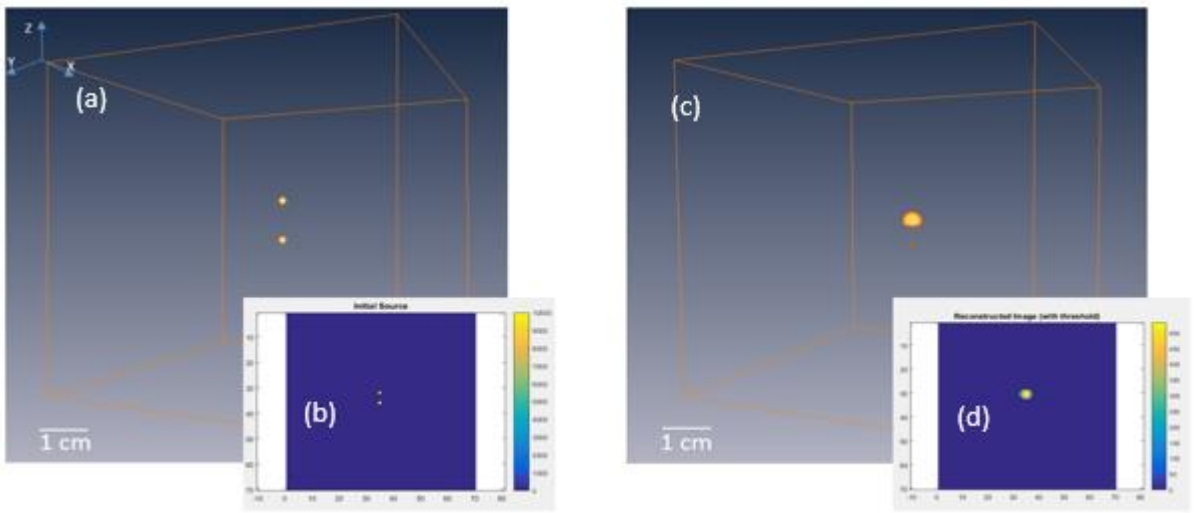

Figure 6: (a) 3D image of initial acoustic source using AMIRA-software. (b) Cross section passing through initial source is plotted in MATLAB. (c) 3D image of reconstructed initial pressure distribution using AMIRA-software. (d) Plane passing through source is plotted for reconstructed pressure distribution. For acoustic sources of 500μm in size and separated by 1mm along the direction of axis of transducer.

The measurement of the reconstructed initial pressure distribution through a line passing through the centre of the source and parallel to z-axis is plotted in Figure 7.

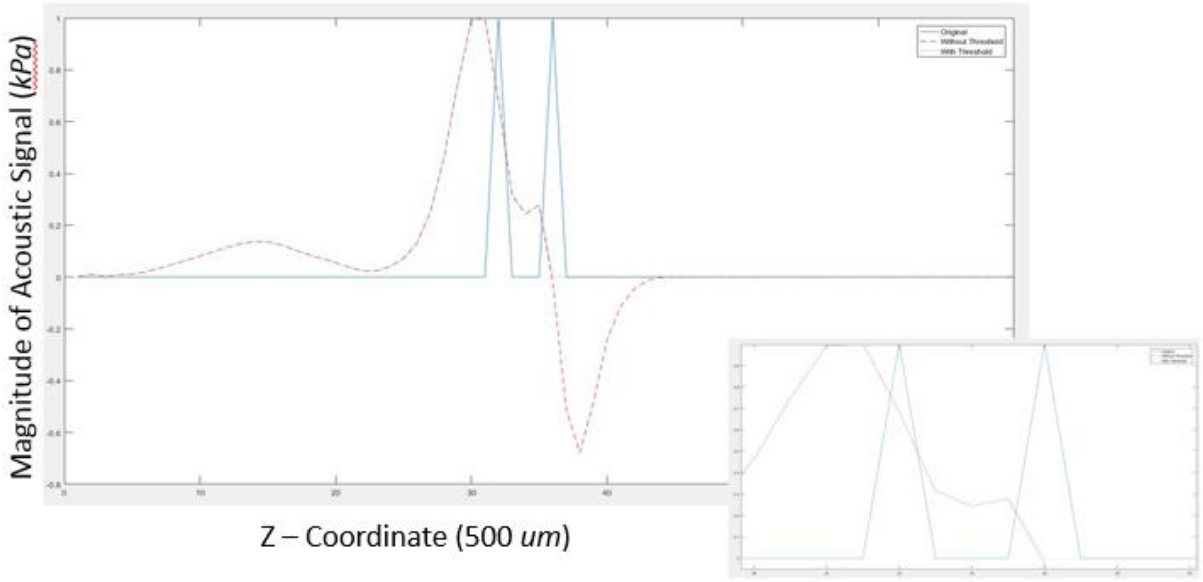

Figure 7: Line plot of measurement in the reconstructed acoustic distribution. Acoustic sources are separated by 1mm along the direction of axis of the transducer. The axes of acoustic magnitude and Y-coordinates are labelled.

Simulation of reconstruction of photoacoustic tomography with 3D image of hair sample as a source of acoustic waves is carried out. Results obtained for the reconstruction of hair sample is given in Figure 8(b). 3D image is created by AMIRA software using the matrix reconstructed by k-wave toolbox. The initial 3D image that is used as the source of acoustic waves is shown in Figure 8(a). Result shows that hair sample is not reconstructed well in the simulation of PAT for hair sample. For improving the reconstruction filtering methods are

applied on the sensor data obtained for the acoustic waves generated from the hair sample. Filtering methods also applied on the reconstructed images also.

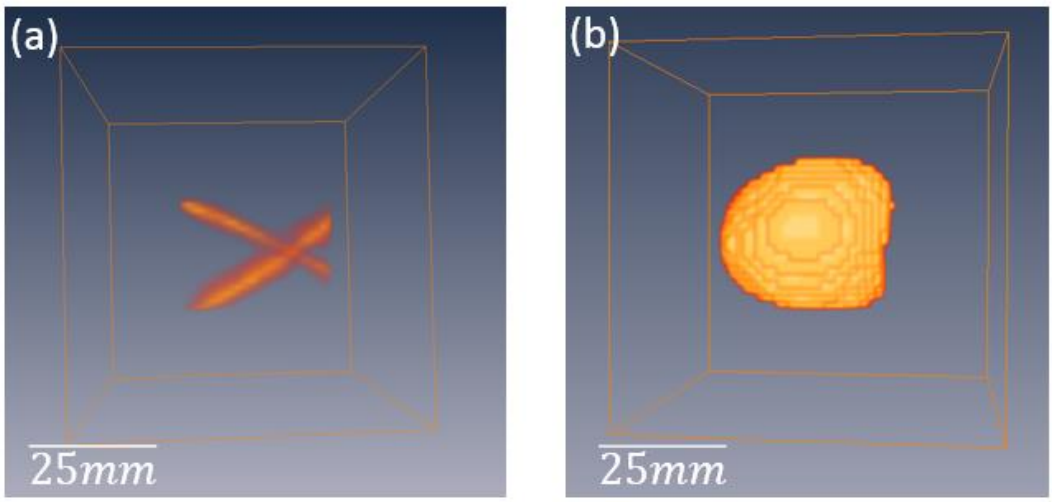

Figure 8: 3D image of hair sample that is used as the source of acoustic waves created by AMIRA software in Figure 8(a). Reconstructed 3D image of hair sample in Figure 8(b).

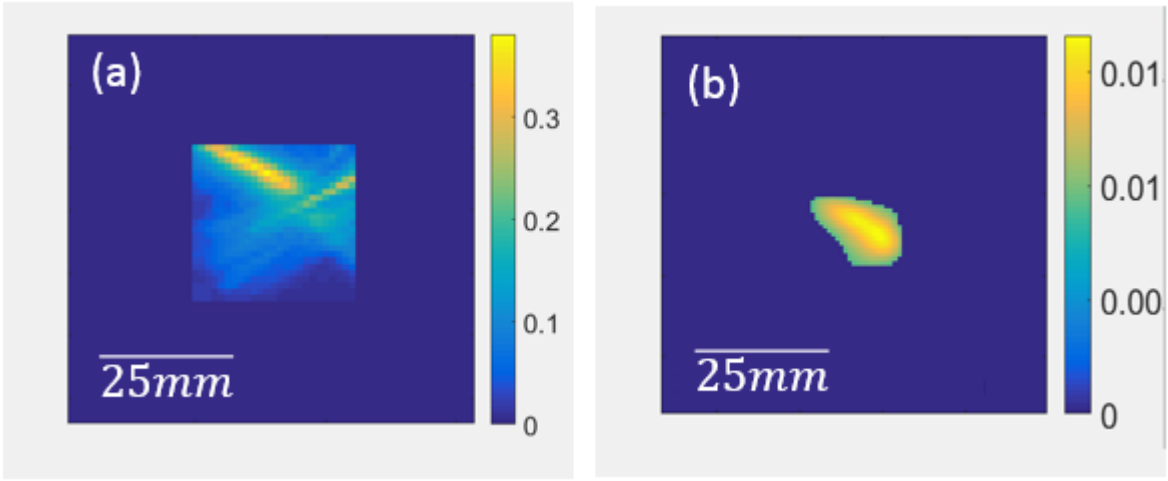

Figure 9: Planar plot of a plane passing through hair sample and parallel to xy plane. Planar plot of image used as source of acoustic waves is shown in Figure 9(a). Planar plot of reconstructed hair sample image is shown in Figure 9(b).

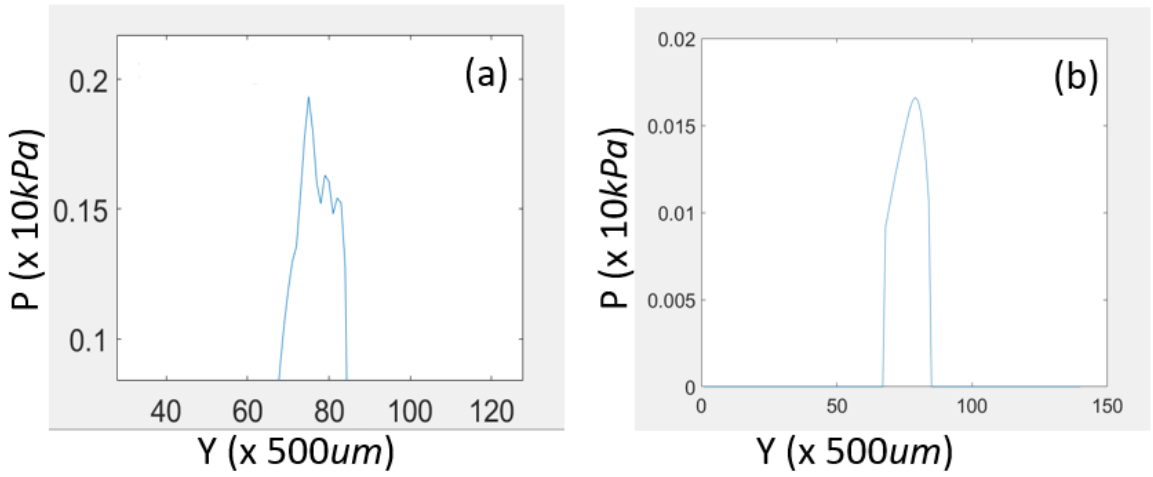

Figure 10: Linear plot along a line that passing through hair sample and lie on a plane parallel to xy plane .Line plot is created using the raw sample hair data in Figure 10(a). Line plot is created using reconstructed acoustic data in Figure 10(b).

4.1 FILTERING METHODS

Image used as source of acoustic waves in the simulation of photoacoustic tomography of hair sample is a raw data obtained for the hair sample using photoacoustic microscopy. This source raw image have a lot of background noise. Background noise also act as a source for acoustic waves. Consequently noises is observed in the reconstructed images. To remove the noises in the reconstructed images, two types of filtering methods is carried out. One of the filtering method applied is standard born ratio technique[6] that is used commonly in imaging technique. This filtering method is applied before the reconstruction. Simulation of acoustic waves is done without the hair sample and acoustic amplitude at the sensor structure is recorded. Acoustic waves is generated only from the background noise in this case. After this hair sample is introduced and simulation of acoustic waves from both hair sample and background noise is done. Division of sensor data obtained for the simulation of acoustic waves generated from the both hair sample and background noise and sensor data obtained for the simulation of acoustic waves generated from the back ground noise only is carried out. Reconstruction is performed using this matrix (matrix obtained after the division) as the recorded sensor data. Results obtained for simulation of PAT using this born-ratio technique is shown in Figure 11. To analyse the result, planar plot and linear plot is taken. Planar plot is taken on the reconstructed image of a plane passing through initial hair sample and parallel to xy plane (Figure 12). Planar plot is taken for source also for comparison. Linear plot along a line that passing through hair sample and lie on a plane parallel to xy plane for reconstructed acoustic data is shown in Figure 13.

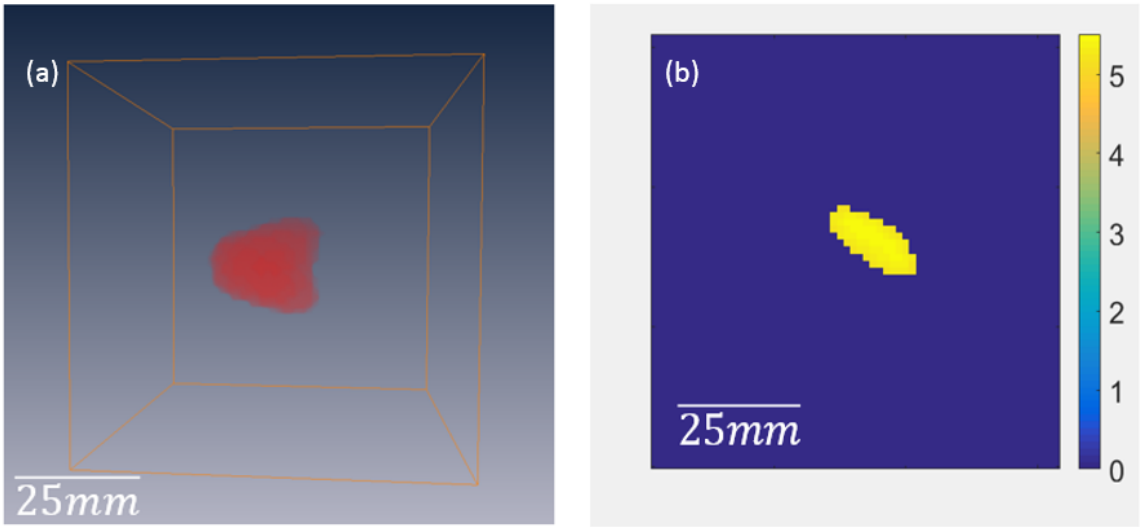

Figure 11: (a) Reconstructed 3D image of hair sample using the born-ratio technique. (b) Planar plot of a plane passing through hair sample and parallel to xy plane. Planar plot of reconstructed hair sample image using born-ratio technique is shown.

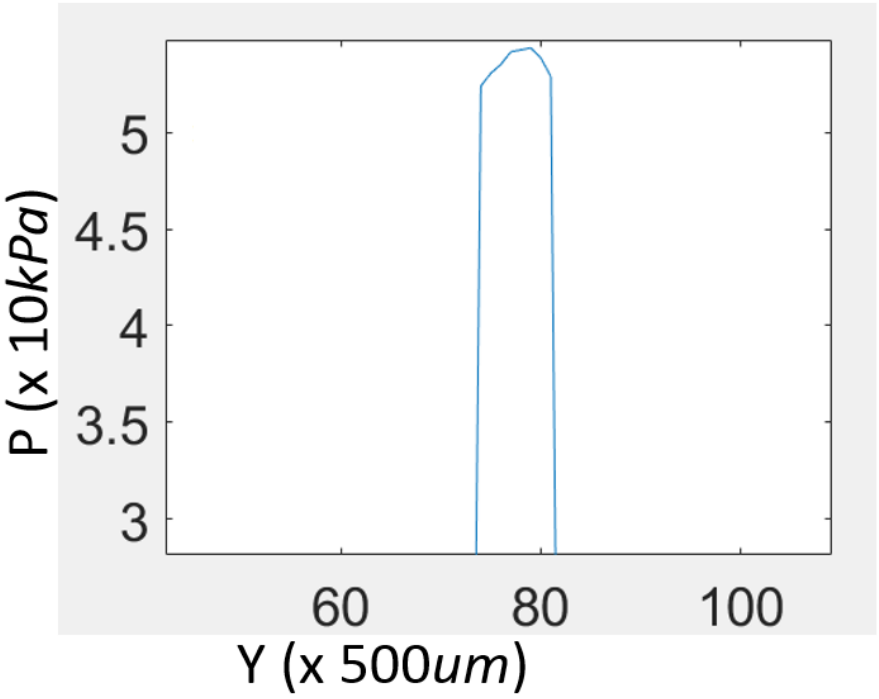

Figure 13: Linear plot along a line that passing through hair sample and lie on a plane parallel to xy plane. Linear plot is plotted on the reconstructed acoustic data using the bon-ratio technique.

As the result observed for the simulation of PAT using born-ratio is not up to the mark. Another filtering method –thresholding filtering - is employed. In this filtering method values less than 30 percentage of maximum acoustic amplitude observed in the matrix obtained as recorded acoustic data is assumed as noise signals. And these values is changed to zero acoustic signals.

Reconstruction is performed using this matrix (Matrix after applying the filtering) as sensor data. This same filtering method is applied on the matrix obtained after the reconstruction also for removing the noise on the reconstructed image. Results obtained for reconstruction using this thresholding filtering method (filtering after the reconstruction also) is shown in figure 14. To analyse the result, planar plot and linear plot is taken. Planar plot is taken on the reconstructed image of a plane passing through initial hair sample and parallel to xy plane (figure 15). Linear plot along a line that passing through hair sample and lie on a plane parallel to xy plane for reconstructed acoustic data is shown in figure 16.

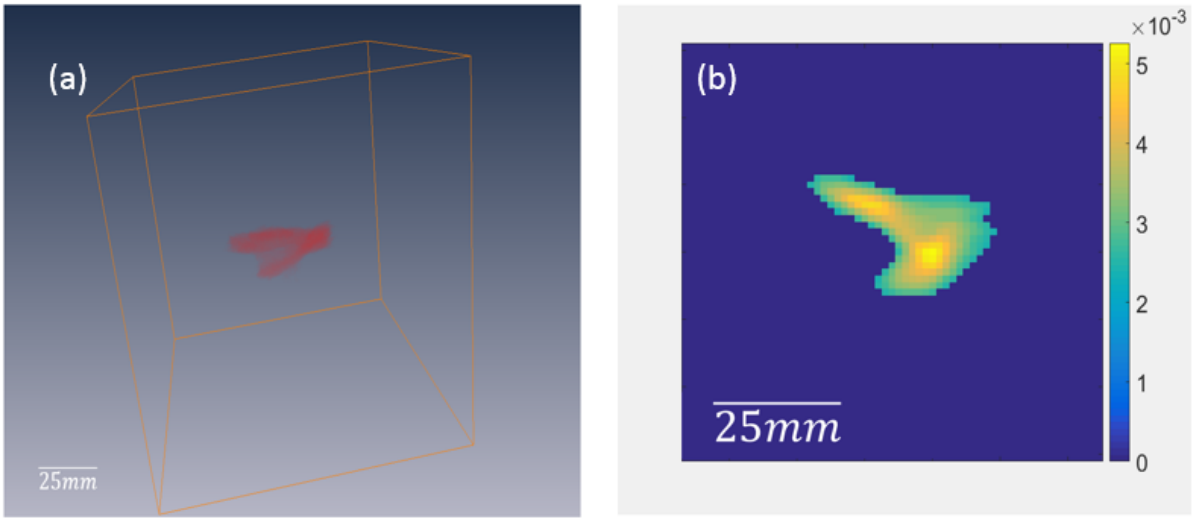

Figure 14: (a) Reconstructed 3D image of hair sample using the threshold technique. Planar plot of a plane passing through hair sample and parallel to xy plane. (b) Planar plot of reconstructed hair sample image using threshold technique is shown.

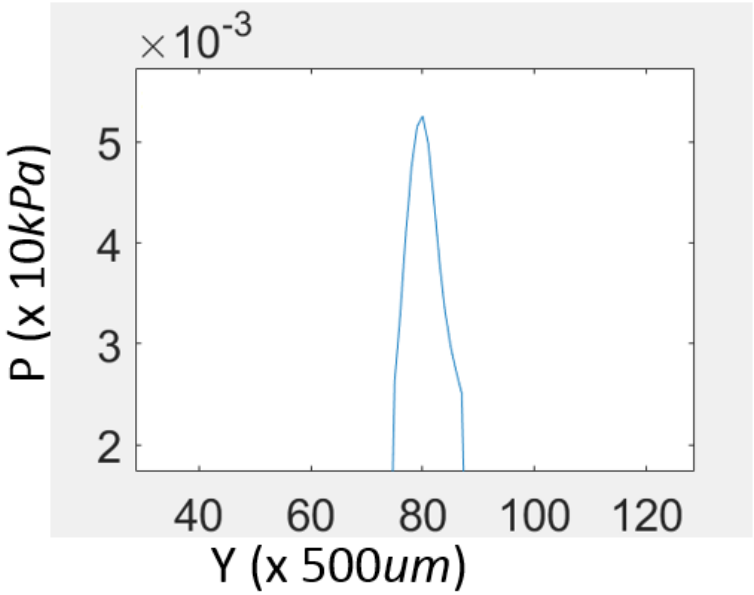

Figure 16: Linear plot along a line that passing through hair sample and lie on a plane parallel to xy plane. Linear plot is plotted on the reconstructed acoustic data using the bon-ratio technique.

5. CONCLUSION

The algorithm for modelling and simulation using k-wave (Acoustic toolbox in k-wave) of PAT experiment that has been being undertaken by our research team to develop a 4D microscopic resolution photoacoustic tomography (4D μ-PAT) imaging system – fundamentally based on photoacoustic effect – with achievable penetration depth (few *cms*),spatial resolution (~200μm) and temporal resolution (10*msec*) is developed. The algorithm is examined 1) for acoustic sources of 250 with spatial resolution of 500μm and the temporal resolution of 50*ns* and it was able to resolve these particles separated by 500μm along the axis of transducer array, 2) For acoustic sources of 500 separated by 1 mm perpendicular to the axis of transducer array, 3) For acoustic source as a 3D image created by data obtained for Photo Microscopy of a hair sample. It was not able to resolve acoustic sources separated in a line perpendicular to the transducer array. Hair sample 3D image is not obtained well when it is reconstructed without using any filtering method. Commonly used born-ratio filtering method applied in the reconstruction. Still the reconstruction performance is not improving munch. Another filtering method is employed using thresholding the values obtained in the simulation, it is observed performance of reconstruction is improved in this filtering method. It is also observed that when the discretization increases the acoustic sources are resolved better.

6. REFERENCES

1 S J Ford, Bigliardi, M Olivo, and D Razansky, Structural and functional analysis of intact hair follicles and pilosebaceous units by volumetric multispectral optoacoustic tomography, J. Invest. Derm. **136**, 753–761 (2016).

2 T F Fehm, X L Deán-Ben, and D Razansky, Four dimensional hybrid ultrasound and optoacoustic imaging via passive element optical excitation in a hand-held probe, Appl. Phys. Lett. **105**(17), 173505 (2014).

3 M Suheshkumar S and H Jiang, Ultrasound (US) transducer of higher operating frequency detects photoacoustic (PA) signals due to the contrast in elastic property, AIP Adv. **6**, 025210 (2016).

4 M Suheshkumar S and H Jiang, Elastic property attributes to photoacoustic signals: an experimental phantom study, Opts. Lett. 39(13), 3970-3973 (2014).

5 L H Wang and S Hu, Photoacoustic tomography: In vivo imaging from organelle to organs, Science 335, 1458 (2012).

6 M Suheshkumar S and P K Yalavarthy, Born-ratio type data normalization improves photoacoustic tomography, Proc. SPIE Med. Imag. **9040**, (2014).

7 B. E. Treeby and B. T. Cox. k-Wave: MATLAB toolbox for the simulation and reconstruction of photoacoustic wave fields. J. Biomed. Opt. **15**(2):021314, 2010.

8 A.G. Bell, On the poduction and reproduction os sound by light. Am. J. Sci. **20**, 305-324 (1880).

9 Manojit Pramanik, Lihong V. Wang, Thermoacoustic & photoacoustic sensing of temperature

10 P. M. Morse and K. U. Ingard, Theoretical Acoustics, Princeton University Press, Princeton, NJ (1968).

11 B. T. Cox and P. C. Beard, "Fast calculation of pulsed photoacousticfields in fluids using kspace methods," J. Acoust. Soc. Am. **177**(6), 3616–3627 (2005).

12 Mingjian Sun, Zhenghua Wu, Ting Liu, Jiajun Hu, Guanqun Wu, and Naizhang Feng, "Time Reversal Reconstruction Algorithm Based on PSO Optimized SVM Interpolation for Photoacoustic Imaging," Mathematical Problems in Engineering, vol. **2015**.(2015).

13 P. Burgholzer, G. J. Matt, M. Haltmeier, and G. Paltauf, "Exact and approximative imaging methods for photoacoustic tomography using an arbitrary detection surface, Physical Review E, (2007).

14 Y. Hristova, P. Kuchment, and L. V. Nguyen, "Reconstruction and time reversal in thermoacoustic tomography in acoustically homogeneous and inhomogeneous media," Inverse Probl. **240**(5), 055006 (2008).